# Axion Star Tidal Effects & Bosenova

高宇 Yu Gao
中国科学院高能物理研究所
IHEP, CAS

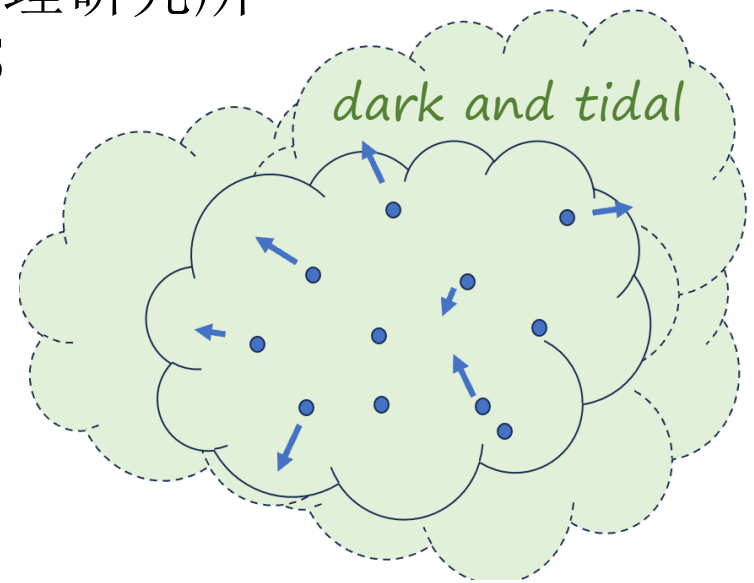


Q. Qiu, Y. Gao, K. Wang, H. Tian, X-M. Yang, Z. Wang, Z.
JCAP 02 (2025) 001
Z.Wang and Y. Gao, Phys.Rev.D 111 (2025) 4, 043042
Z.Wang and Y. Gao, 2508.14535

大连 2025/09/21

- Brief remarks
- DM gravity on stars: kinetic heating
- Binary disruption: form factor for fuzzy objects
- Quick story about axion & DM
- Dilute stars
- Binary limits for axion stars & miniclusters.
- Bosenova in Miniclusters

# Axion can form miniclusters & stars

Sensitivity on via density/gravity structural patterns can shed some light on boson DM properties.

Miniclusters:

Post-inflationary scenario causes inhomogeneities.
A naïve estimate on the clump masses:

$$M \approx \frac{4\pi}{3}(1+\delta)\bar{\rho}H(T_{osc})^{-3}$$

Or solve the density fluctuation's equation

$$\ddot{\delta} + 2H\dot{\delta} + \left(\frac{c_s^2 k^2}{a^2} - 4\pi G_N \bar{\rho}_a\right)\delta = 0$$

$$c_s^2 \approx \frac{k^2}{4m_a^2 a^2}$$

1207.3124

See: 1404.1938 1810.11468 1911.07853 2006.08637

Or use N-body simulation.

1911.09417 2101.04177 2207.11276 2402.18221

Axion stars:

See review:
Braaten & Zhang, 19'
J. Niemeyer, 19'

Localized (soliton) solutions under self-interaction / gravity

Oscillons ($\dot{m}_a > 0$): astro-ph/9311037
Boson star (w gravity) 1406.6586

$$i\dot{\psi} = -\frac{\nabla^2\psi}{2m} - Gm^2\psi\int d^3x' \frac{\psi^*(\mathbf{x}')\psi(\mathbf{x}')}{|\mathbf{x}-\mathbf{x}'|} + \frac{\partial}{\partial\psi^*}V_{nr}(\psi,\psi^*)$$

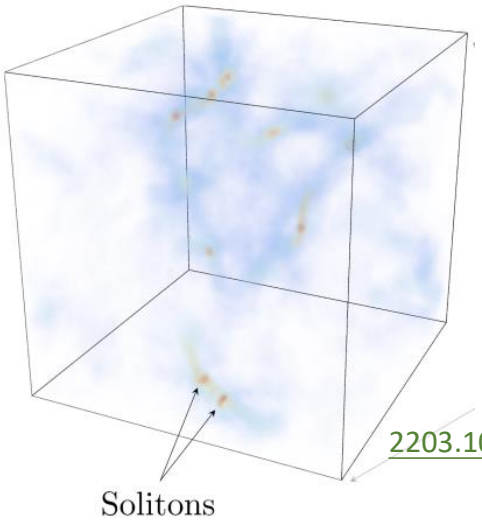


2203.10100

# Gravitational interests in dark clumps/solitons

**All evidences of DM are gravitational:** should gravity tell us more?

>> Preferred as a **cored** DM halo <<

Galaxy scale dynamics:
Disk thickening, stellar streams
Church, J. P. Ostriker, and P. Mocz, 18'
Amorisco and A. Loeb, 18'
excludes $m < 10^{-22}$ eV

Granularity above the de Broglie wavelength ~ $2\pi/mv$ L.Hui, 16'
exclusion limit $m \rightarrow 10^{-21}$eV

Relaxation of old clusters, exclusion limit $m \rightarrow 10^{-20}$~$10^{-19}$eV
Bar-Or, Fouvry, and Tremaine, 19'
Marsh and Niemeye, 19'
Wasserman, 19' etc.

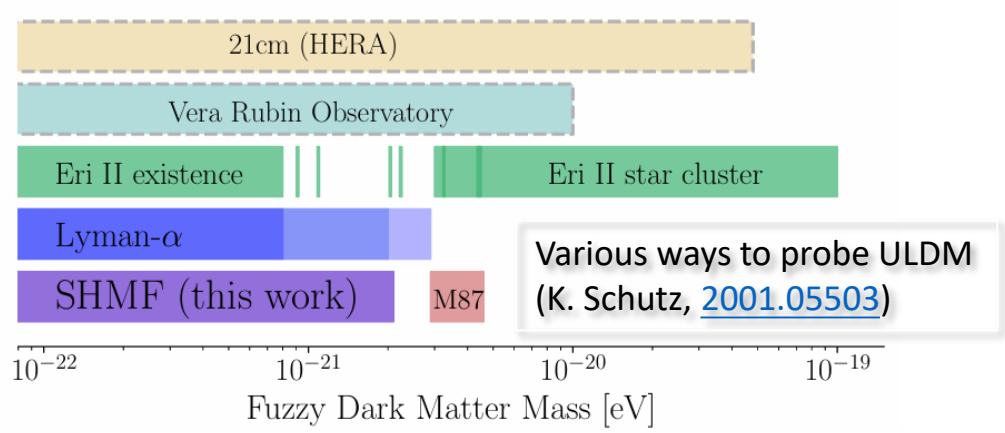


Various ways to probe ULDM
(K. Schutz, 2001.05503)

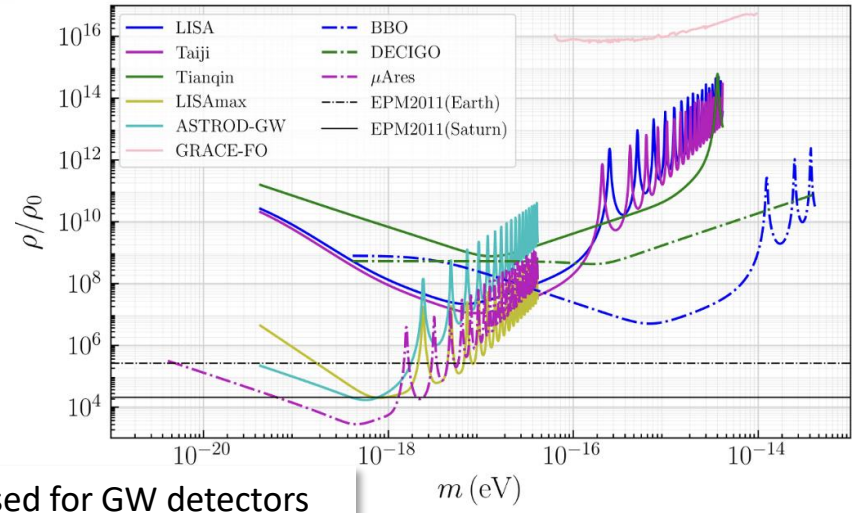


Proposed for GW detectors
(summary from 2404.04333)

# The tidal relaxation

DM granules ($\lambda \sim (mv)^{-1}$) passing by a star perturb the star's velocity, raising the (average) stellar velocity dispersion:

$$\Delta v_\star^2 \propto \left(\frac{v_\star}{v_{DM}}\right)^4 \frac{t}{m_{DM}^3 r_{1/2}^4}$$

1. Density granularity (by solitons) above its coherent scale creates a randomized, noise-like gravitational potential.

2. Randomized tidal perturbations drive stars away from their orbits, leading to eventual evaporation of the system

3. Most effective on systems comparable or larger than the granularity size.

4. Unlike WIMPs, solitons have a macroscopically significant mass and contribute to relaxation.

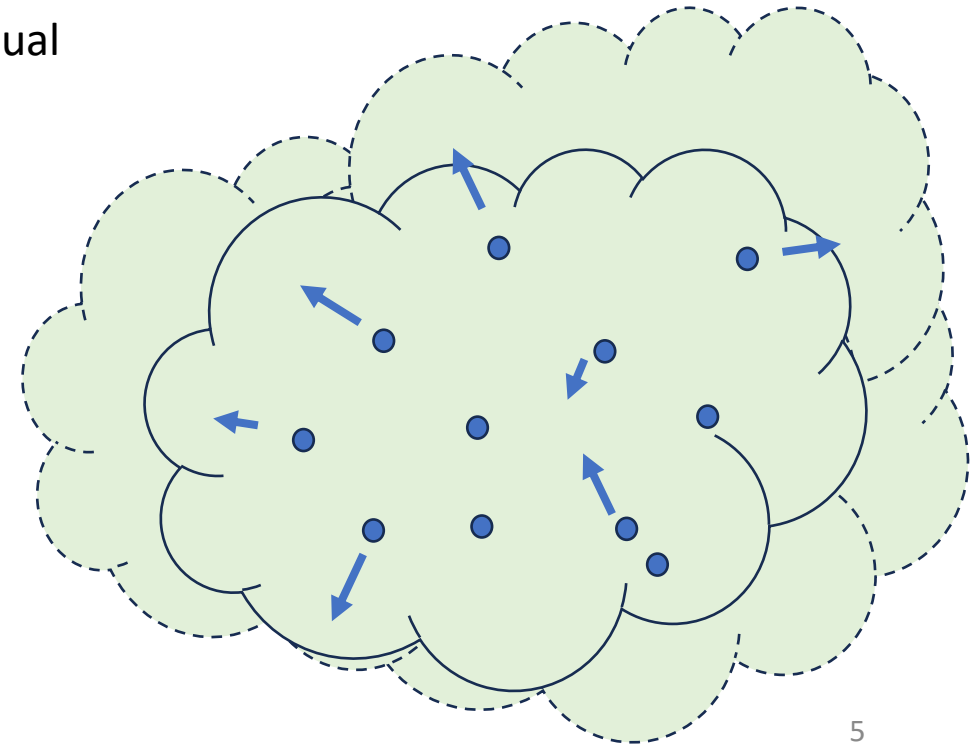

# DM kinetic heating

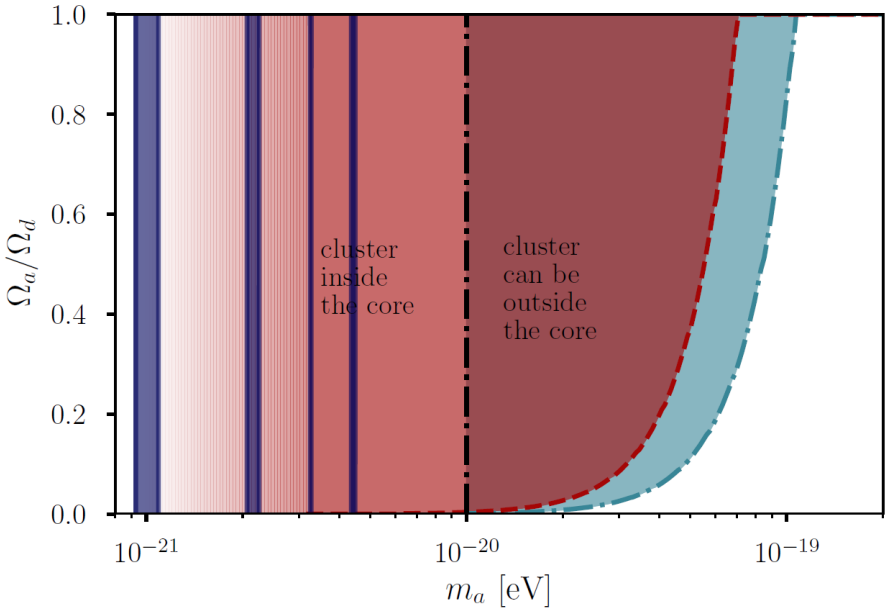


Axion DM granularity contributes to Cluster Relaxation

Relaxation for **Eridanus II,** see Marsh and Niemeyer, 19'
See `revised constraints', Chiang et.al: 2104.13359

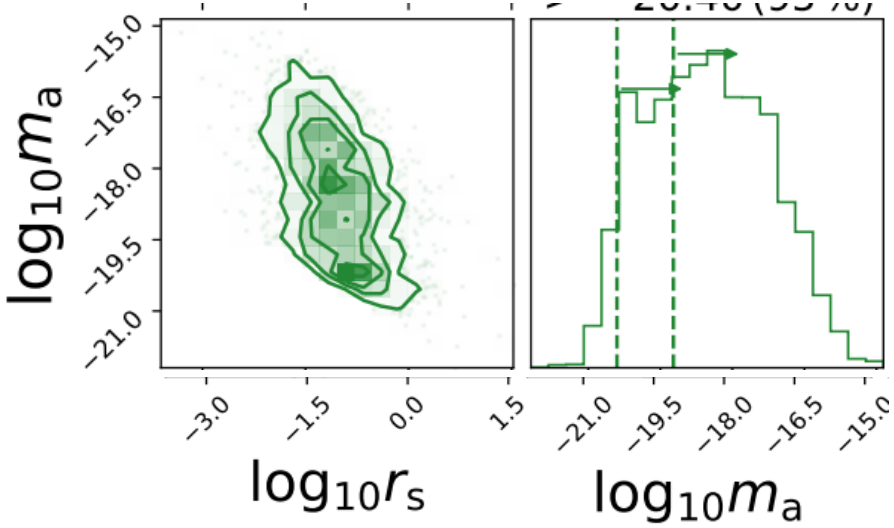


**The MUSE-Faint survey** (2101.00253 )

Quote: …. These limits are equivalent to a fuzzy-dark-matter particle mass $\mathbf{m_a > 4*10^{-20}\ eVc^{-2}}$."

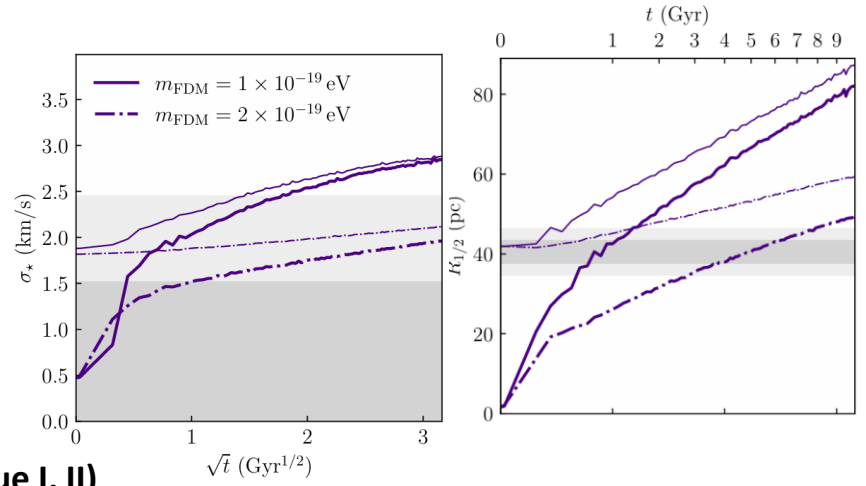


**Ultra-faint dwarves (Segue I, II)**

Dalal & Kravtsov, 2203.05750, quote: … derive a lower limit on the dark matter particle mass of $\mathbf{m_{FDM} > 3x10^{-19}\ eV}$ **at 99% C.L.**[via simulated stellar motion]

# Smaller (<< kpc) objects for small structures?

Our Galaxy hosts a population of very wide (up to ~ 1pc) binaries/candidates

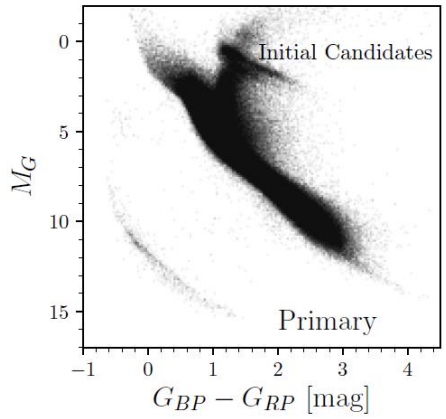


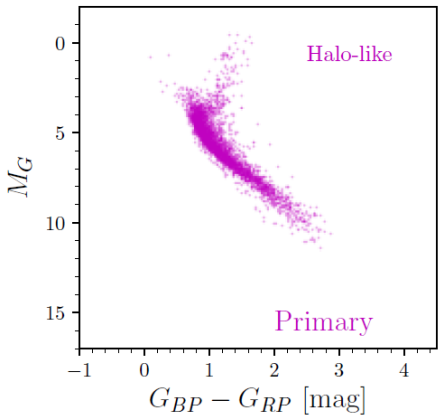


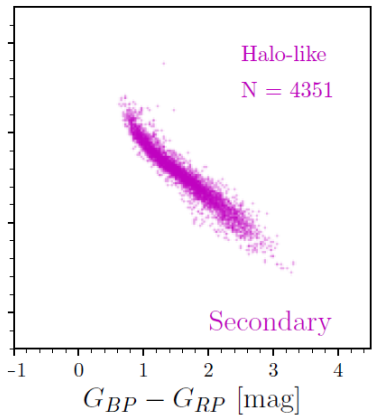


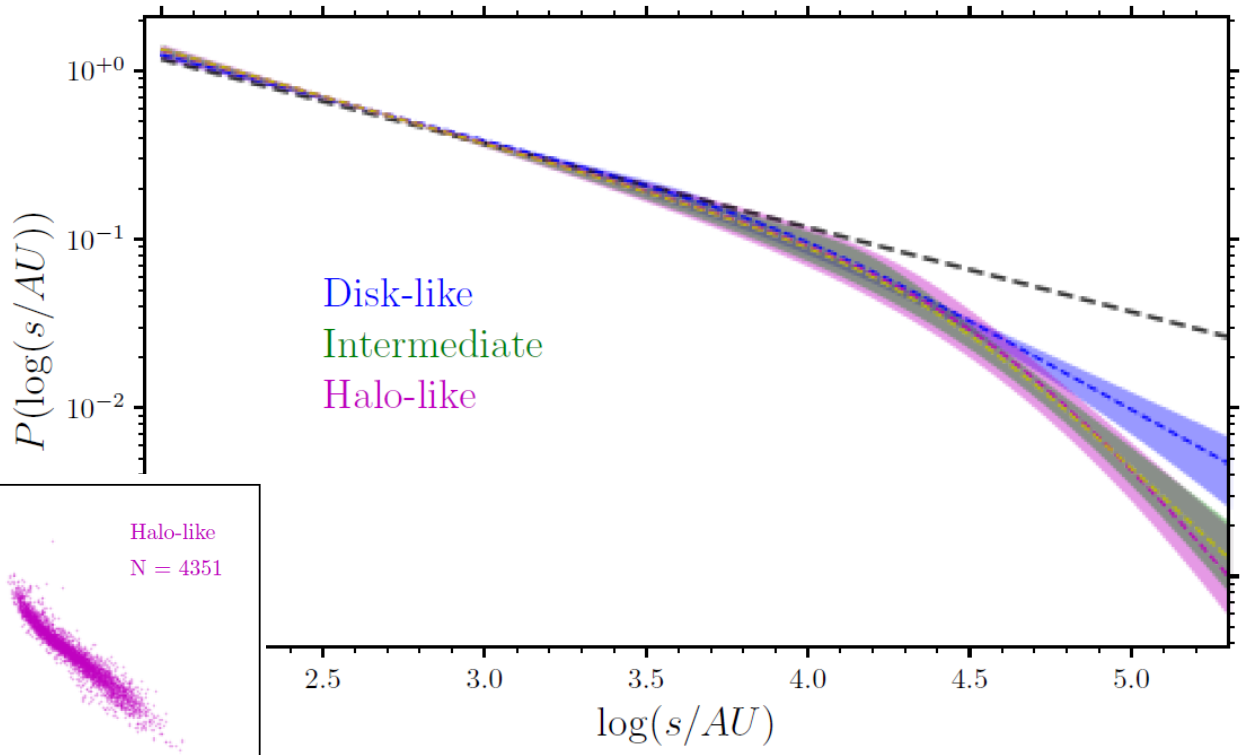


Tian, et.al. 19', from GAIA data

**Evaporation**: increment of energy leads to final disruption of the binary system.

For binary evaporation, the two-body system can be reduced
to a well-defined single-body problem (plus some input from its COM motion)

$$\Delta E = \mu \vec{v_r} \cdot \Delta \vec{v_r} + \frac{1}{2}\mu (\Delta \vec{v_r})^2$$

$\nabla\,\Phi$ drives the CM's random walk (can be small compared to $v_{cm}$~$10^{-3}c$)
Tidal acceleration should be in proportional to $\partial \wedge \partial\,\Phi$

$$\Delta \vec{v}_r = \Delta \vec{v}_1 - \Delta \vec{v}_2,$$

$$\frac{\langle \Delta \vec{v_r}^2 \rangle}{T} = \frac{1}{T}\left(\langle \Delta \vec{v}_1^2 \rangle + \langle \Delta \vec{v}_2^2 \rangle - 2\langle \Delta \vec{v}_1 \cdot \Delta \vec{v}_2 \rangle\right)$$

$$\frac{\langle \Delta E \rangle}{T} = \mu \frac{\vec{v}_r \cdot \langle \Delta \vec{v}_r \rangle}{T} + \frac{1}{2}\mu \left( \frac{\langle \Delta \vec{v}_1^2 \rangle}{T} + \frac{\langle \Delta \vec{v}_2^2 \rangle}{T} - \frac{2\langle \Delta \vec{v}_1 \cdot \Delta \vec{v}_2 \rangle}{T} \right)$$

$\langle\ \rangle$ : spectral averaging over the soliton ensemble.
1/T : time averages… should also take account of the binary's Keplerian motion.

# Slow orbit: wide binaries

$$\frac{\lambda_{\rm DM}}{v} \ll T \ll \frac{2\pi}{\omega_b}$$

For wide binaries, $v_r / v_{cm} \sim 10^{-3}$. For a longer orbit period than the time scale of potential variations, one can take the ensemble average first, and leave the orbital parameters as constants.

Velocity change driven by the potential's gradient

$$\Delta\vec{v} = -i\int_0^T dt \int \frac{\vec{k}d^3k d\omega}{(2\pi)^4}\Phi(\vec{k},\omega)e^{i(\vec{k}\cdot\vec{r}-\omega t)}$$

To include the gravitational potential variations, expand out r(t) that travels across the DM background

$$\vec{r}(t) \approx \vec{r}_0 + \vec{v}_0 t + \int_0^t ds(t-s)\dot{\vec{v}}(s)$$

$$\exp\left[i(\vec{k}\cdot\vec{r}-\omega t)\right] = \exp\left[i\vec{k}\cdot\left(\vec{r}_0 + \vec{v}_0 t + \int_0^t d\tau(t-\tau)\dot{\vec{v}}(\vec{r}_0+\vec{v}_0\tau,\tau)\right) - i\omega t\right]$$

$$\approx e^{i\vec{k}\cdot(\vec{r}_0+\vec{v}_0 t)-i\omega t}\left[1 + i\vec{k}\cdot\int_0^t d\tau(t-\tau)\dot{\vec{v}}(\vec{r}_0+\vec{v}_0\tau,\tau)\right]$$

**The first term will vanish after the ensemble average. The only contribution comes from the second term**

Expand out the equation

$$\Delta\vec{v} = i\int_0^T dt\int_0^t d\tau(t-\tau)\int\frac{\vec{k}d^3kd\omega}{(2\pi)^4}\int\frac{(\vec{k}\cdot\vec{k'})d^3k'd\omega'}{(2\pi)^4}\Phi(\vec{k},\omega)\Phi^*(\vec{k'},\omega')e^{i\vec{k}\cdot(\vec{r_0}+\vec{v_0}t)-i\omega t}e^{-i\vec{k'}\cdot(\vec{r_0}+\vec{v_0}\tau)+i\omega'\tau}$$

And make use of the relation:

$$\left\langle\Phi(\vec{k},\omega)\Phi^*(\vec{k}',\omega')\right\rangle = (2\pi)^4C_\Phi(\vec{k},\omega)\delta^3(\vec{k}-\vec{k}')\delta(\omega-\omega')$$

We can make it an integral over the correlation function.

$$\langle\Delta\vec{v}\rangle = \int_0^T dt\int_0^t d\tau\int\frac{d^3kd\omega}{(2\pi)^4}\vec{k}^2C_\Phi(\vec{k},\omega)\frac{\partial}{\partial\vec{v_0}}e^{i(\vec{k}\cdot\vec{v_0}-\omega)(t-\tau)}$$

The 1st order `diffusion' coefficient:

$$D[\Delta\vec{v}] = \frac{\langle\Delta\vec{v}\rangle}{T} = -\frac{1}{2}\int\frac{\vec{k}d^3kd\omega}{(2\pi)^3}\vec{k}^2C_\Phi(\vec{k},\omega)K'_T(\omega-\vec{k}\cdot\vec{v_0})$$

where $K'_T(\omega) = \dfrac{\omega T\sin(\omega T)-2[1-\cos(\omega T)]}{\pi\omega^3T}$

# Correlation functions

Spectra of the two-point correlation functions for the density $\rho$ and gravitational potential $\Phi$

$$\langle \rho(\vec{r},t)\rho(\vec{r'},t')\rangle \equiv C_\rho(\vec{r}-\vec{r'},t-t')$$
$$\langle \Phi(\vec{r},t)\Phi(\vec{r'},t')\rangle \equiv C_\Phi(\vec{r}-\vec{r'},t-t')$$

Fourier trans.

$$C_\rho(\vec{r},t) = \int \frac{d^3k d\omega}{(2\pi)^4} C_\rho(\vec{k},\omega) e^{i(\vec{k}\cdot\vec{r}-\omega t)}$$

By Poisson Eq. $\nabla^2\Phi = 4\pi G\rho$

$$C_\Phi = 16\pi^2 G^2 k^{-4} C_\rho$$

$$F(\vec{v}) = \frac{\rho_0}{(2\pi\sigma^2)^{\frac{3}{2}}} e^{-\frac{v^2}{2\sigma^2}}$$

Small-sized solitons are more likely virialized so we assume a Maxwellian velocity distribution.

Performing an average over their *v*-distribution

$$C_\rho(\vec{k},\omega) = \frac{1}{m_s}\int d^3r d^3r' d^3v dt \rho(\vec{r})\rho(\vec{r'})F(\vec{v})e^{-i\vec{k}\cdot(\vec{r}+\vec{r'}+\vec{v}t)}e^{i\omega t}$$

$$C_\rho(\vec{k},\omega) = \frac{1}{m_s}\rho^2(\vec{k})\rho_0\sqrt{\frac{2\pi}{k^2\sigma^2}}e^{-\frac{\omega^2}{2k^2\sigma^2}}$$

$\rho(k)$ is the F.T. of the soliton profile

Quadratic terms dominate kinetic energy growth.

$$\frac{1}{2}\mu\left(\frac{\langle\Delta\vec{v}_1^2\rangle}{T}+\frac{\langle\Delta\vec{v}_2^2\rangle}{T}-\frac{2\langle\Delta\vec{v}_1\cdot\Delta\vec{v}_2\rangle}{T}\right)$$

An accurate and concise form factor is obtained after lengthy algebra

$$\frac{\langle\Delta\vec{v}_1^2\rangle}{T}=\int\frac{\vec{k}^2d^3k}{(2\pi)^3}C_\Phi(\vec{k},\vec{k}\cdot\vec{v}_1)$$

$$\frac{\langle\Delta\vec{v}_2^2\rangle}{T}=\int\frac{\vec{k}^2d^3k}{(2\pi)^3}C_\Phi(\vec{k},\vec{k}\cdot\vec{v}_2)$$

$$\frac{\langle\Delta\vec{v}_1\cdot\Delta\vec{v}_2\rangle}{T}=\int\frac{\vec{k}^2d^3k}{(2\pi)^3}C_\Phi(\vec{k},\vec{k}\cdot\vec{v}_c)\cos[\vec{k}\cdot(\vec{r}_1-\vec{r}_2)]$$

[Use approximation]

$$v_c\gg v_r,\ v_1\approx v_2\approx v_c$$

Finally, the tidal heating rate:

Remember $|r_1\text{-}r_2|\sim 2a$, soliton size becomes relevant.

$$\frac{\langle\Delta E\rangle}{T}=\sqrt{\frac{2}{\pi}}\frac{\mu\rho_0G^2}{m_s\sigma}\int\frac{d^3k}{k^3}\rho^2(\vec{k})e^{-\frac{(\vec{k}\cdot\vec{v}_c)^2}{2k^2\sigma^2}}2\left(1-\cos\left[\vec{k}\cdot(\vec{r}_1-\vec{r}_2)\right]\right)$$

This convolution factor takes care of scale dependence and reveals the difference btw the 2-body relative motion and the Brownian walk of a single-point particle (COM) under tidal perturbations.

# Size effect in evaporation time scale

$$\frac{\langle \Delta E \rangle}{T} = \frac{8\pi\mu\rho_0 G^2 m_s}{v_c} A\left(r_x, r_y, r_z, R, \frac{v_c}{\sigma}\right)$$

Re-define our integrals and make a similar-looking to the classical formula

The relaxation time: $$t_d = \frac{|E_0|}{\left(\frac{dE}{dt}\right)_0} \int_0^1 \frac{dx}{A\left(\frac{R}{a_0}x, \frac{v_c}{\sigma}\right)}$$

Solition size matters!

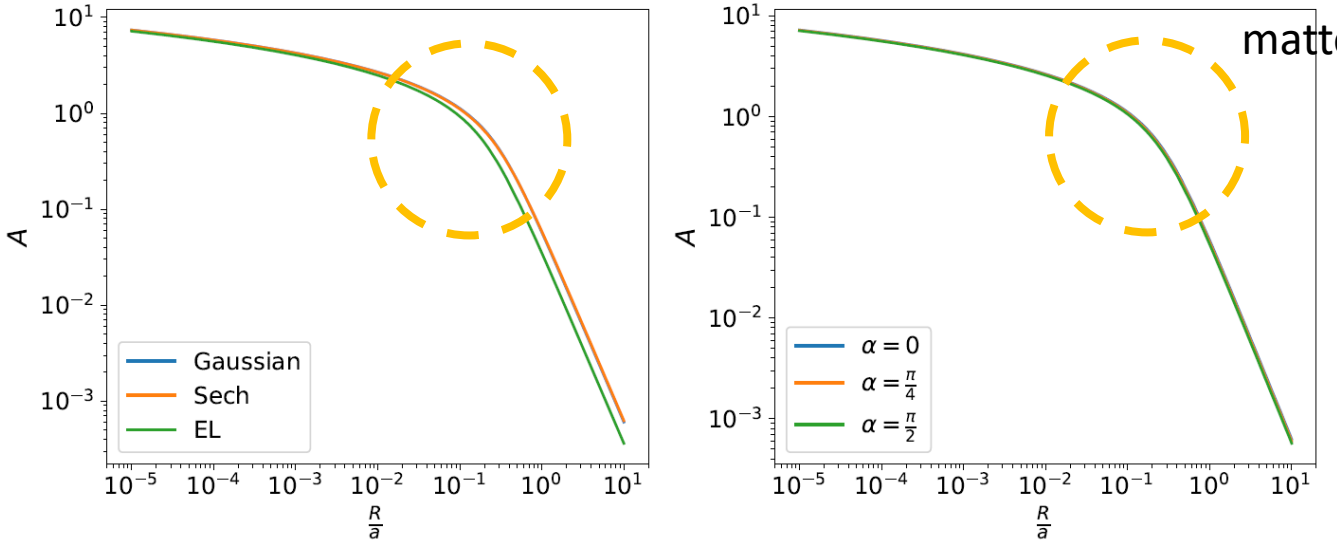


$$A = \frac{1}{\sqrt{2\pi}} \frac{v_c}{\sigma} \int_0^{+\infty} \frac{dk}{k} \frac{\rho^2(k)}{m_s^2} \int_{-1}^{1} dx e^{-\frac{v_c^2 x^2}{2\sigma^2}} \left[1 - J_0\left(k\sqrt{r_x^2 + r_y^2}\sqrt{1-x^2}\right)\cos(k r_z x)\right]$$

# GAIA catalog: halo-like wide binaries

- Select old binary candidates with large tangential velocity
- Select candidates with a low probability of being aligned by chance
- Veto candidates with close companions, many neighbors (N<2)
- Exclude candidates containing white dwarves

El-Badry and H.-W. Rix, Mon. Not. Roy. Astron. Soc. 480, 4884 (2018)

2000+ candidates pass selection cuts out of 62990 from GAIA data

Gaia Collaboration, Astronomy & Astrophysics 649, A9 (2021), 2012.02036.

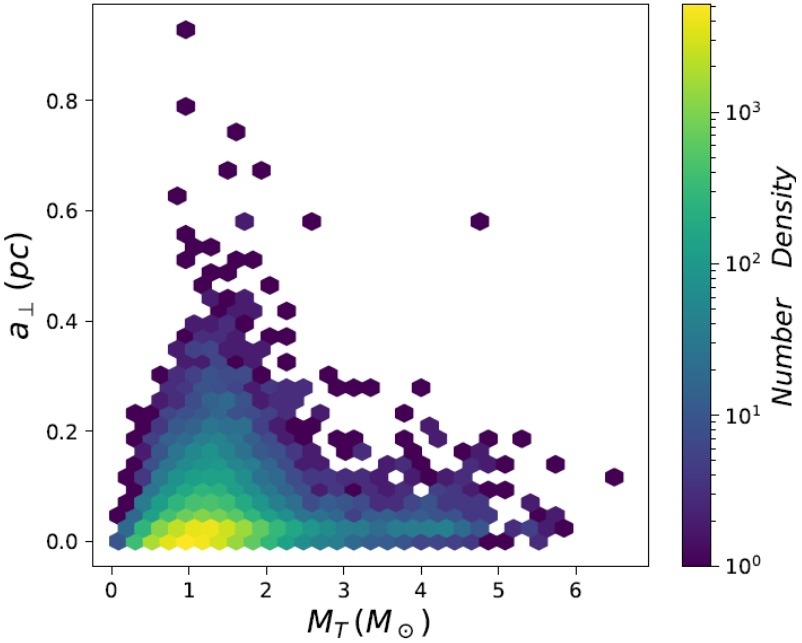


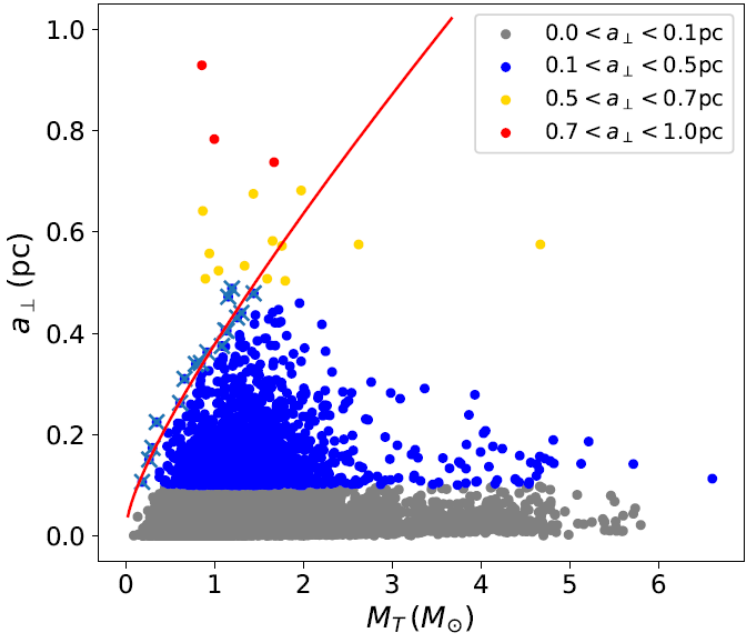

Select high-prob. candidates with large separation and relatively lower mass.

Require their average evaporation to be longer than 10 Gyr

$$\langle t_d \rangle \equiv \frac{1}{N} \sum_i t_{d,i} \ < 10 \text{ Gyr},$$

| Source id1 | Source id2 | parallax1 | parallax2 | g mag1 | g mag2 | R chance align | $M_1$ | $M_2$ | $M_T$ | $a_\perp$(pc) |
|---|---|---|---|---|---|---|---|---|---|---|
| 1312689344512158848 | 1312737894822499968 | 3.375 | 3.310 | 12.07 | 17.21 | 0.000996 | 0.950 | 0.483 | 1.432 | 0.675 |
| 6644959785879883776 | 6644776515331203840 | 2.007 | 2.354 | 17.85 | 18.00 | 0.0462 | 0.440 | 0.412 | 0.851 | 0.929 |
| 2305945096292235648 | 2305945538674043392 | 2.366 | 2.316 | 15.74 | 17.30 | 1.53e-09 | 0.518 | 0.373 | 0.891 | 0.508 |
| 2127864001174217088 | 2127863726296352256 | 1.370 | 1.363 | 13.64 | 15.60 | 0.0357 | 0.924 | 0.741 | 1.665 | 0.737 |
| 577970351704355072 | 580975626220823296 | 3.117 | 3.021 | 16.35 | 17.47 | 0.0850 | 0.484 | 0.452 | 0.937 | 0.557 |
| 1401312283813377536 | 1401310698969746944 | 1.244 | 1.234 | 16.97 | 18.92 | 0.0113 | 0.631 | 0.409 | 1.040 | 0.523 |
| 1559537092292382720 | 1559533965556190848 | 1.209 | 1.224 | 13.63 | 15.03 | 0.00142 | 1.117 | 0.854 | 1.971 | 0.682 |
| 5476416420063651840 | 5476421406528047104 | 1.204 | 1.214 | 13.66 | 15.46 | 0.0834 | 1.016 | 0.775 | 1.791 | 0.503 |
| 4004141698745047040 | 4004029857796571136 | 5.104 | 5.100 | 14.09 | 16.07 | 0.00492 | 0.580 | 0.412 | 0.992 | 0.783 |
| 6779722291827283456 | 6779724009814201984 | 1.575 | 1.579 | 17.72 | 18.79 | 0.00712 | 0.484 | 0.378 | 0.862 | 0.641 |
| 3594791561220458496 | 3594797539814936832 | 1.065 | 1.069 | 14.44 | 16.31 | 0.0763 | 0.917 | 0.731 | 1.649 | 0.582 |
| 3871814958946253312 | 3871818601078520192 | 1.449 | 1.499 | 15.66 | 17.13 | 0.0188 | 0.676 | 0.657 | 1.333 | 0.533 |
| 2379971950014879360 | 2379995177198014976 | 1.604 | 1.588 | 14.21 | 16.58 | 0.0270 | 0.876 | 0.712 | 1.588 | 0.507 |
| 6826022069340212864 | 6826040868412655872 | 2.379 | 2.373 | 11.76 | 14.05 | 0.0987 | 1.016 | 0.738 | 1.754 | 0.572 |
| 5798275535462480768 | 5798276325736369024 | 1.247 | 1.261 | 13.32 | 13.76 | 0.000536 | 1.443 | 1.176 | 2.619 | 0.575 |

TABLE I: (Catalog I). High probability halo-like wide binaries with $a_\perp > 0.5\,\text{pc}$ and $M_T < 3\,M_\odot$.

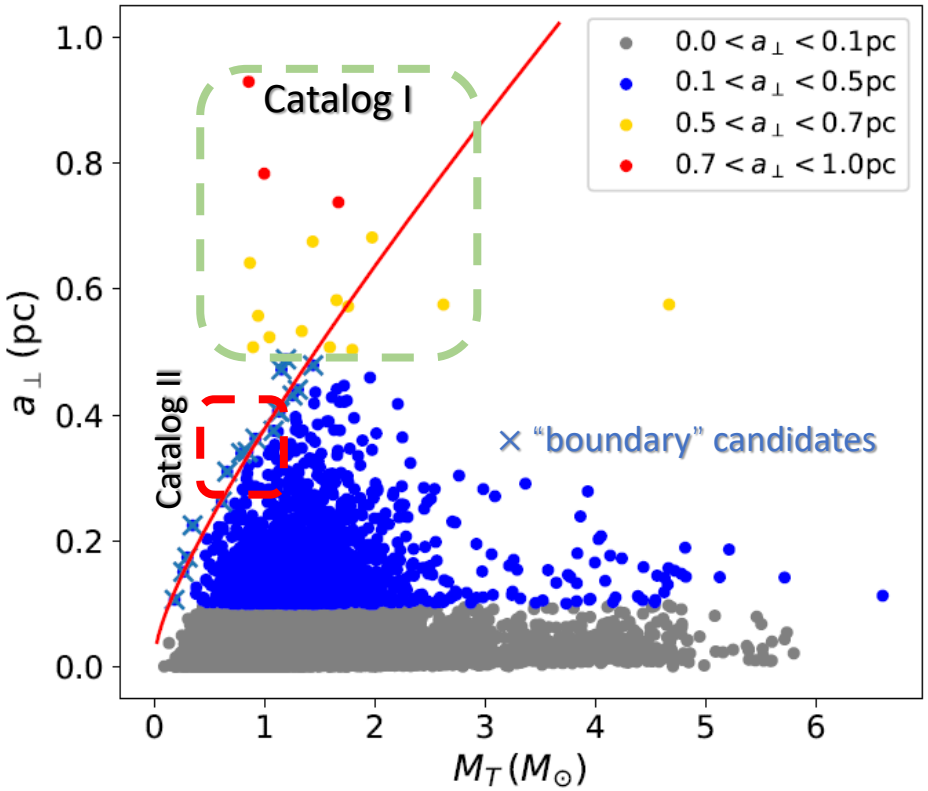


- Binaries shift left-ward over time under tidal perturbations
- A $t_d$=10 Gyr curve and its soliton configuration ($m_s$, R) is ***disfavored*** if lots of candidates reside on its left/top side
- (red line) on the boundary of populated region corresponds to $t_d$= 10 Gyr with ($m_s$=9.3$m_\odot$, R=0.03pc)

JCAP 02 (2025) 001

Catalog I & II limits for $t_d = 10^{10}$ yr under solitons' tidal perturbation.
(Blue bands) solutions for ALPs with potential: $V(a) \sim -m_a^2 f_a^2 \cos(a/f_a)$

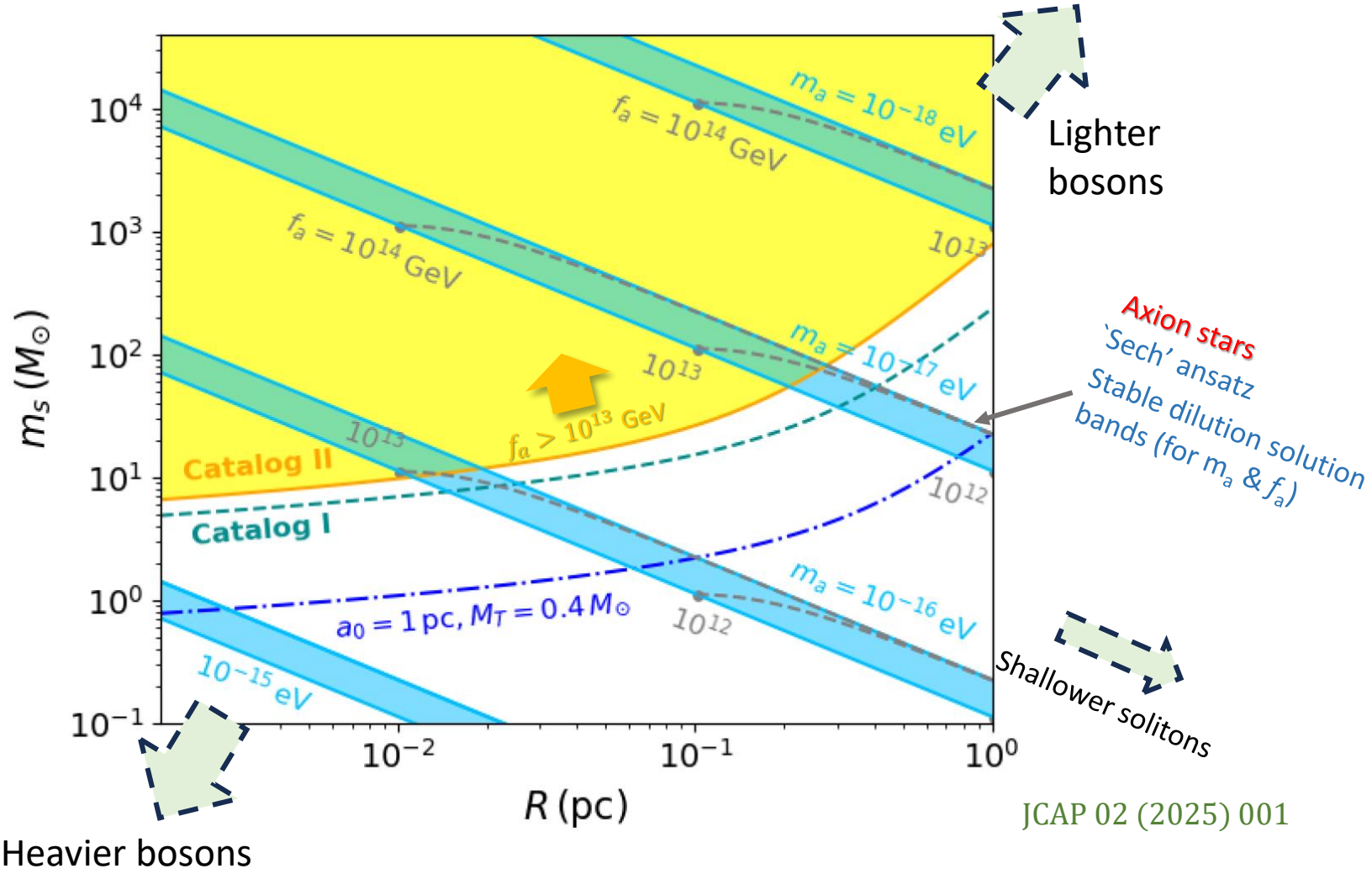


JCAP 02 (2025) 001

# Brief notes about axion stars

Derive the non-relativistic Hamiltonian and find a minimum.

Real scalar Lagrangian: $\mathcal{L} = \sqrt{-g}\left[\frac{1}{2}g^{\mu\nu}\nabla_\mu a \nabla_\nu a - V(a)\right]$

Nonrelativistic approximation: $a(\vec{x},t) = \frac{1}{\sqrt{2m_a}}\left(e^{-im_a t}\psi(\vec{x},t) + e^{im_a t}\psi^*(\vec{x},t)\right)$

$$n(\mathbf{x}) = \psi^*(\mathbf{x})\psi(\mathbf{x}) \text{ and } \rho(\mathbf{x}) = m\,\psi^*(\mathbf{x})\psi(\mathbf{x})$$

Nonrelativistic Lagrangian, with $g_{00} = 1 + 2\phi_N$:

$$\mathcal{L}_{nr} = \frac{i}{2}\left(\dot{\psi}\psi^* - \psi\dot{\psi}^*\right) - \frac{1}{2m}\nabla\psi^*\cdot\nabla\psi - V_{nr}(\psi,\psi^*) - m\,\psi^*\psi\,\phi_N(\psi^*,\psi)$$

Stable solution: presence of a minimum of the reduced Hamilitonian.

Use dimensionless variables:

$$\tilde{H} = \frac{\sqrt{|\lambda|^3}}{m_a^2\sqrt{G}} H\,,$$
$$\tilde{N} = m_a\sqrt{G|\lambda|}\,N\,,$$
$$\tilde{R} = m_a^2\sqrt{\frac{G}{|\lambda|}}\,R\,,$$

Rescaled energy:

$$\tilde{H} = a\frac{\tilde{N}}{\tilde{R}^2} - b\frac{\tilde{N}^2}{\tilde{R}} - c\frac{\tilde{N}^2}{\tilde{R}^3}$$

Plug into ansatz:

$$a = \frac{12+\pi^2}{6\pi^2}\,,\; b = \frac{6\left[12\zeta(3)-\pi^2\right]}{\pi^4}\,,\; c = \frac{\pi^2-6}{8\pi^5}$$

At low density, the axion number stays unchanged. For fixed N~, H~ can minimize at a certain radius

$$\tilde{R} = \frac{a \pm \sqrt{a^2 - 3bc\tilde{N}^2}}{b\tilde{N}}$$

Growth beyond this point destabilizes the axion star.

# Solution stability at fixed N~

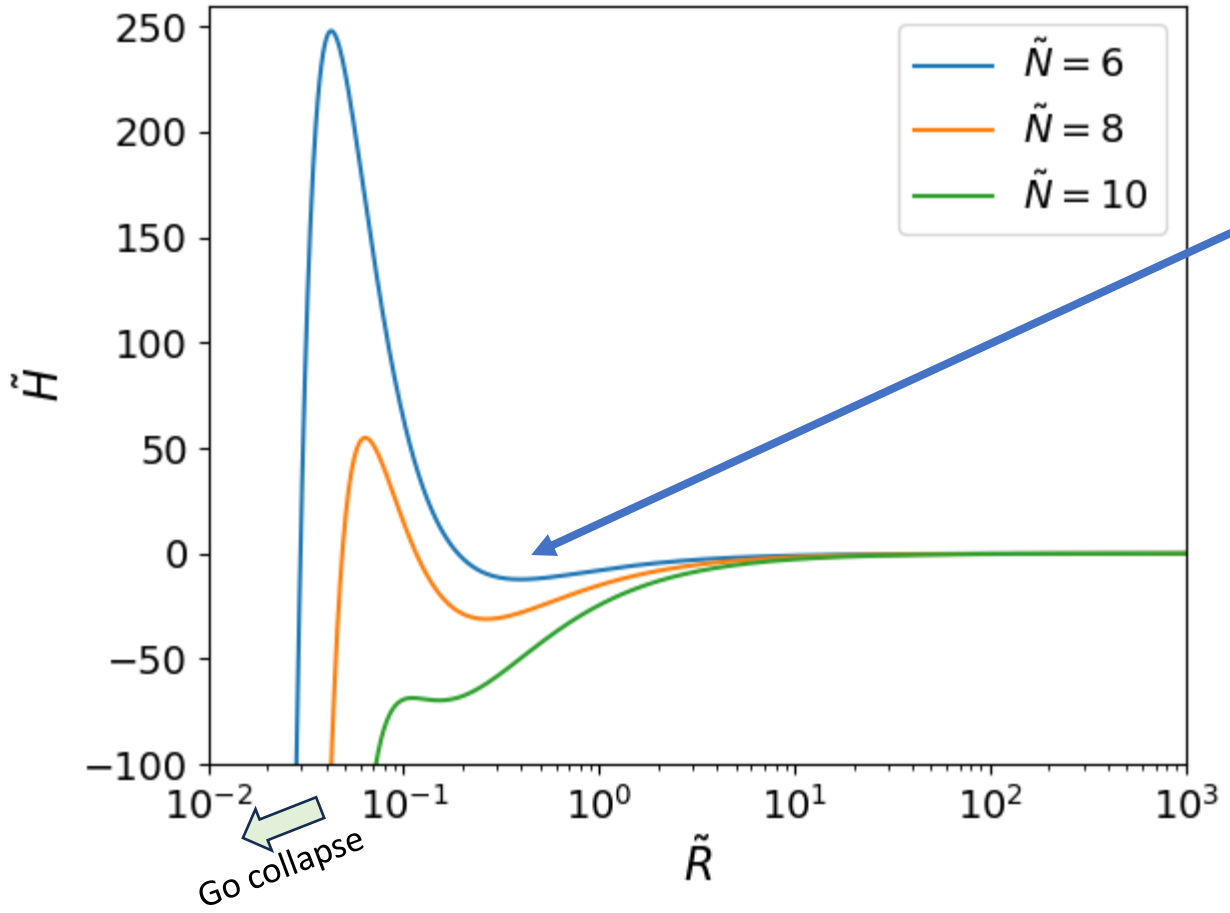


Presence of a local minimum: **stable** solution

Stable dilute axion star solution exists if

$$\tilde{N} \leq 10.12$$

For larger axion star mass, it will collapse to form a dense axion star

(Blue bands) show stable dilute-star solutions

for ALP potential: $V(a) \sim -m_a^2 f_a^2 \cos\left(\frac{a}{f_a}\right)$

Larger $f_a$ reaches denser solutions (left).

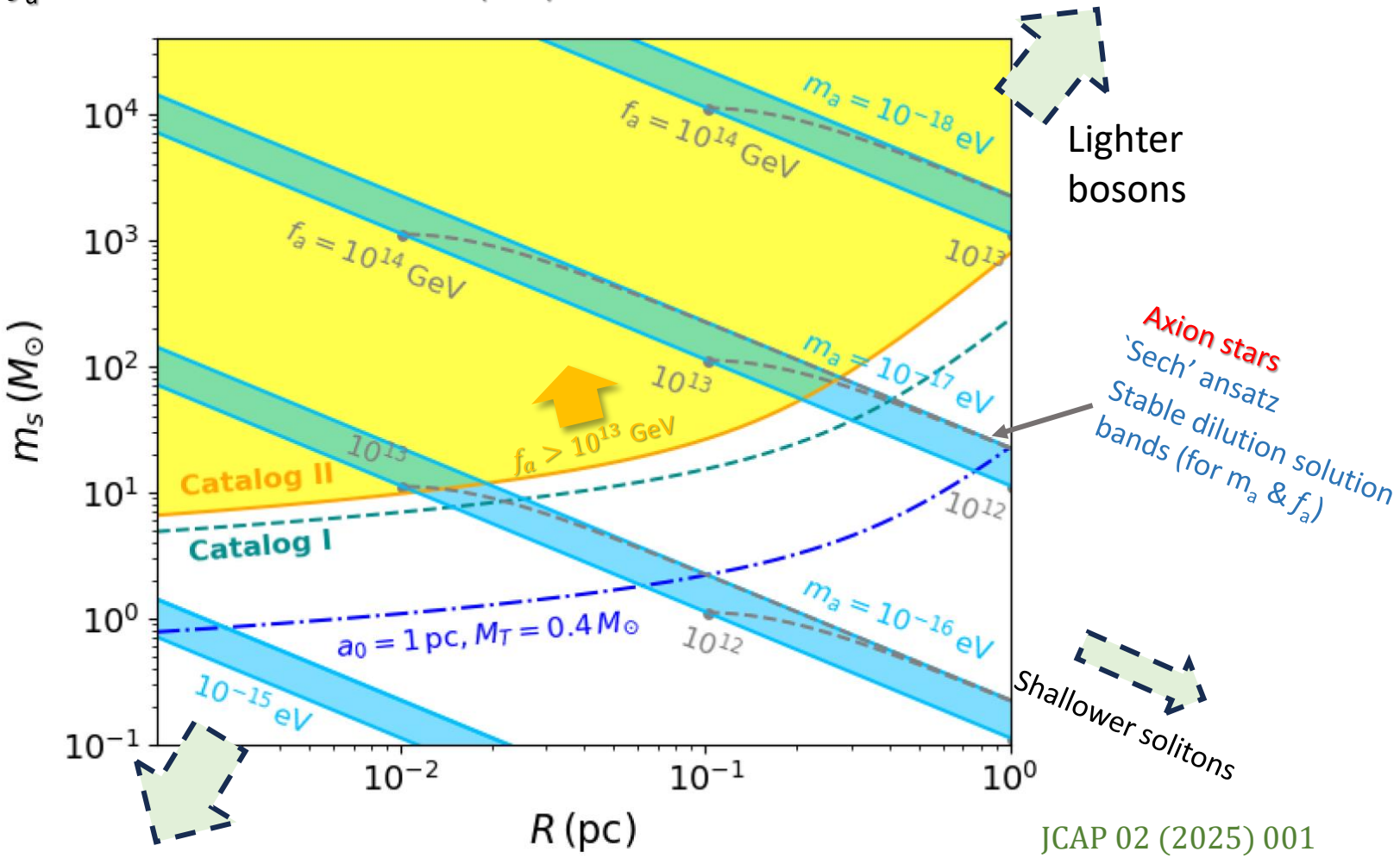


JCAP 02 (2025) 001

# Binary disruption bounds: for ALP minicluster halos

More `realistic' axion distributions from numeric and semi-analytic calculations

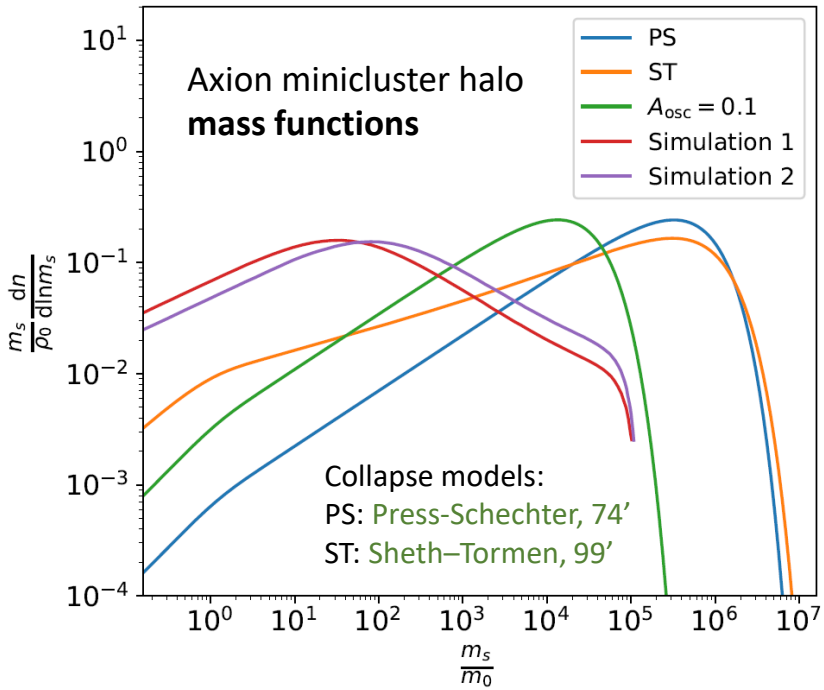


$$m_0 = 281 M_\odot \left(\frac{m_a}{10^{-16}\,\mathrm{eV}}\right)^{-\frac{3}{2}} \frac{g_{*S}(T_{\rm osc})}{g_{*S}(T_0)} g_*^{-\frac{3}{4}}(T_{\rm osc})$$

Denser models of MCH indicate for more significant disruption effect.

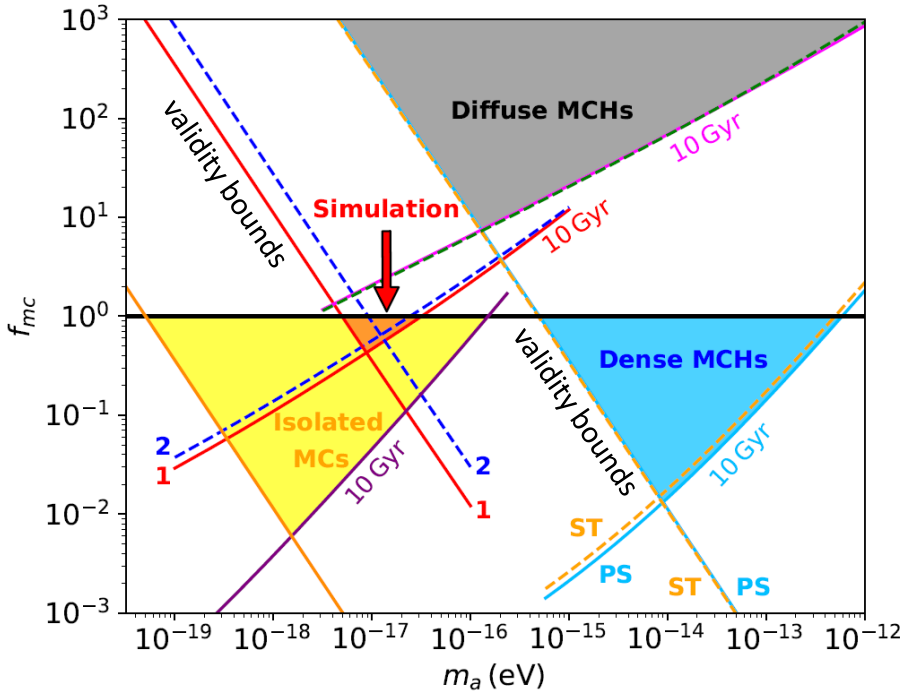


Condensation (soliton size) models,

$$\rho(r) = \frac{\rho_c}{\frac{r}{r_s}\left(1+\frac{r}{r_s}\right)^{-2}} \cdot \frac{200}{3} \frac{c^3}{\ln(1+c) - \frac{c}{1+c}}$$

Diffuse: low concentration, c ~ 10, larger MC size
Dense: high concentration, c ~ $10^4$, compact MCs
Isolated: MCs do not clump into MCHs

Phys.Rev.D 111 (2025) 4, 043042

# Axion star forms inside a `minicluster' and feeds on its host.

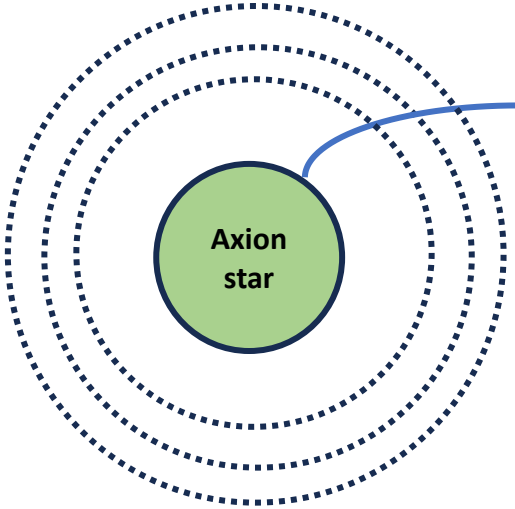


Fuzzy axion halo
(minicluster)
has a nonzero velocity

Axion star: large number of axions stay on the same (BEC) state $\psi_S$

`BEC in virialized DM halos'
see Levkov, Panin, Tkachev, 18',
formation under self-gravity

Axion star will further grow and potential trigger run-away self-interaction (instability).

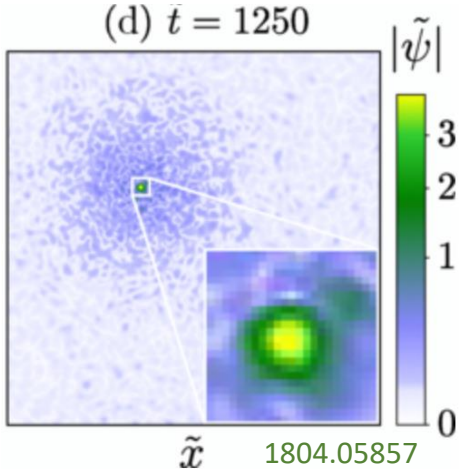


Star growth calculation:
halo axion capture by BEC via self-gravity.
see Chan, Sibiryakov, Xue, 24'

Potential signals?

***Q1:*** Instability requires the incorporation of axion's self-interaction: dilute stars :gravity and self-interaction equilibrium.

***Q2:*** Mapping growth stability into axion parameters space $(m_a, f_a)$ requires incorporation of the self-interaction potential

A quantum calculation for axion capture $\psi_g + \psi_g \to \psi_S + \psi_g$ via self-interaction potential $V \sim a^4$

$$S = \int \mathrm{d}^4x \left( \frac{1}{2}\partial_\mu a \partial^\mu a - \frac{1}{2}m_a^2 a^2 - \frac{1}{24}\lambda a^4 \right)$$

$$S_g = \int \mathrm{d}t\mathrm{d}^3\vec{x} \left( i\psi_g^* \partial_t \psi_g + \frac{1}{2m_a}\psi_g^* \nabla^2 \psi_g - \frac{\lambda}{16m_a^2}|\psi_g + \psi_s|^4 \right)$$

Nonrelativistic limit and take $\psi_S$ as a bkg state

$$|\mathcal{M}_{g+g\to g+s}|^2 = \left| \int \mathrm{d}^3x\mathrm{d}t \, \langle f|\mathcal{H}_{\mathrm{int}}|i\rangle \right|^2 = \frac{\lambda^2}{64m_a^4} \left| \int \mathrm{d}^3x\mathrm{d}t \, \langle f|\psi_s^*|\psi_g|^2\psi_g|i\rangle \right|^2$$

$\psi_S$: BEC's common soliton state

$$\psi_s(\vec{x}, t) = \chi(r)e^{-i\epsilon_s t}$$

$\chi(r)$ takes stable solution ansatzes.

$\psi_g$: `gas' state in virialized minicluster

$$\psi_g(\vec{x}, t) = \frac{1}{\sqrt{V}} \sum_{\vec{k}} a_{\vec{k}} \varphi_{\vec{k}}(\vec{x}) e^{-i\epsilon_{\vec{k}} t}$$

$$\varphi_{\vec{\kappa}}\left(\vec{\xi}\right) = e^{i\vec{\kappa}\cdot\vec{\xi}}\Gamma\left(1 - \frac{i\beta}{\kappa}\right) e^{\frac{\pi\beta}{2\kappa}} {}_1F_1\left[\frac{i\beta}{\kappa}, 1, i\left(\kappa\xi - \vec{\kappa}\cdot\vec{\xi}\right)\right]$$

Scattering states under Coulomb potential

*Amp* calculation includes both axion self-interaction and self-gravity, 2508.14535

Typical horizon collapse minicluster mass (host mass, $M_0$)

$$M_0 = \frac{4\pi^4}{3}\frac{\bar{\rho}_a(t_0)R_{\rm osc}^{-3}}{H^3(t_{\rm osc})} = 1.235\times10^{-9}\,M_\odot\left(\frac{m_a}{10^{-5}\,{\rm eV}}\right)^{-0.561}$$

Axion star initial mass (by num. simulation, $M_{s0}$), from Levkov et.al. 2024

$$M_{s0} = 8.384\times10^{-11}\,M_\odot\times$$
$$\alpha_0\left[\delta^3(1+\delta)\right]^{\frac{1}{6}}\left(\frac{m_a}{10^{-5}\,{\rm eV}}\right)^{-1}\left(\frac{M_0}{M_\odot}\right)^{\frac{1}{3}}$$

Axion star max stable mass (dilute stars, $M_{\rm max}$)

$$M_{\rm max} = 1.089\times10^{-11}\,M_\odot\left(\frac{m_a}{10^{-5}\,{\rm eV}}\right)^{-2}$$

Self-interaction growth time to reach $M_{\rm max}$

$$t_{c,\lambda} = \frac{1}{\Gamma_\lambda} = \frac{1541\,{\rm Gyr}}{\left[\delta^3(1+\delta)/10^8\right]^{\frac{5}{3}}}\times$$
$$\left(\frac{\alpha_0}{\sqrt{2/5}}\right)^2\left(\frac{\alpha(\nu,\tilde{N})}{60}\right)^{-1}\left(\frac{m_a}{10^{-5}\,{\rm eV}}\right)^{-1.374}$$

$t_{\rm growth}$ < AoU (yellow shaded region)

Bosenovae for QCD axion (large δ) and ALPs (quite common) in our Universe. For details see 2508.14535

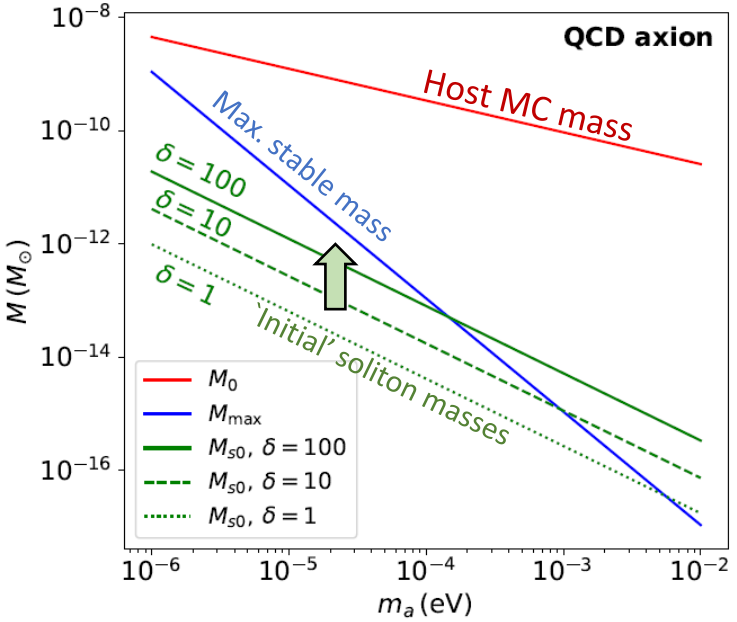


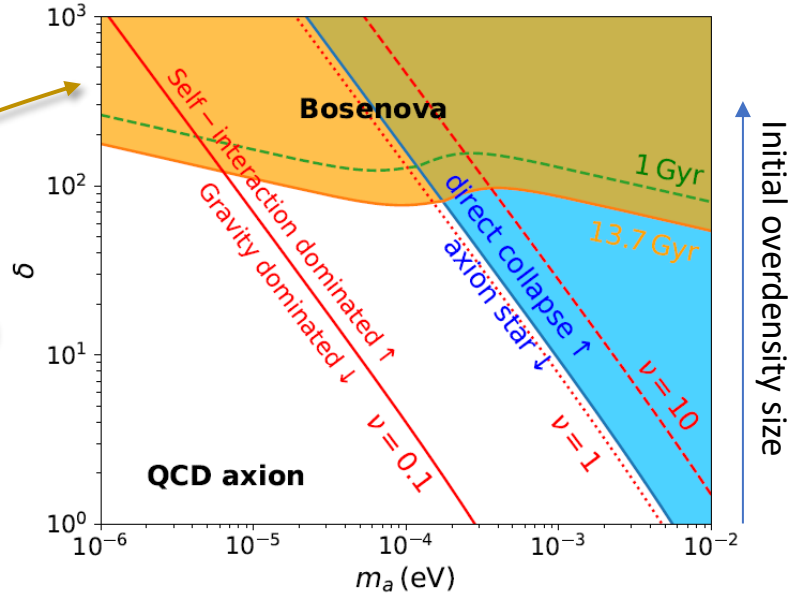

# Take home messages

- Interest in DM's gravitational imprints is on the rise.
- We provide an *analytic* form factor of binary evaporation by randomly distributed, spatially extended objects. For dilute axion stars, sensitivity extends into heavier ALP mass range $10^{-17} < m_a < 10^{-15}$ eV.
- GAIA data contain some *2000+ high-probability, halo-like, a>0.1 pc candidates* → sensitivity to DM tidal disruptions.
- Sophiscated DM mass distributions: Tidal disruption limits are relevant.
- Axion stars go bosenova: possible for both QCD axion/ALP dark matter.

# Backups

- (Summary version of) the Axion DM story:

QCD axion

The SM contains chiral-U(1) breaking effects and develops $V(\bar{\theta})$.

$\bar{\theta}$ is a naturally ~O(1) fundamental parameter in SM.

Non-detection of neutron EDM requires $V(\bar{\theta})$ sitting right at $\bar{\theta} = 0$. (Strong CP)

New field charged under $U(1)_{PQ}$ -> rotational dof contributes to chiral anomaly.

$\bar{\theta} \to \bar{\theta} + a/f$ helps rolling to $\bar{\theta} = 0$.

DM

$a$ gets mass from $V(\bar{\theta})$ and qualifies as a `wavy' dark matter candidate.

axion field has stable SP-equ solutions under self-gravity & interaction -> axion star

# Axion: a story from basic symmetries

Lee & Yang, 56'; Wu, 57'

- Weak int. violates both *P* and *CP*.

Cronin, Fitch, 64'

- *CP* symmetry in strong interaction?

$$\mathcal{L} \supset -\frac{1}{4}G^2 + \frac{\theta g_s^2}{32\pi^2}G\tilde{G}$$

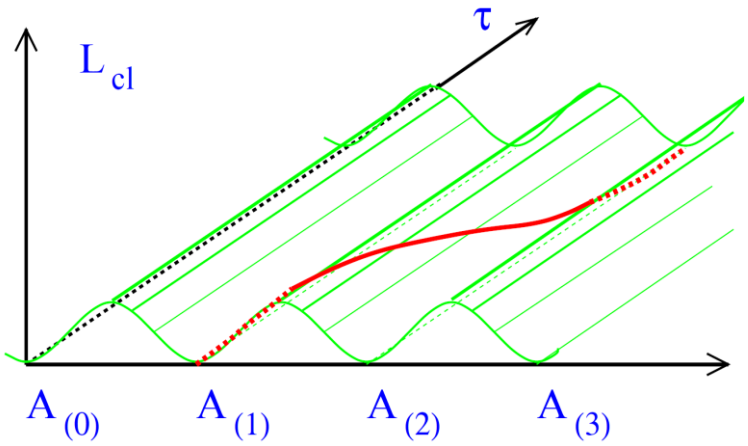


In the SM, CP is broken by QCD ($\theta_{QCD}$), as super-selection rule of QCD's instanton connected vacua

$$|\theta\rangle = N\sum e^{i\theta n}\,|n\rangle$$

Classical (PG) vacua connected by instantons, hep-ph/0009136
Vacuum min. energy @ $\theta = 0$, with Dirac spectrum assumptions (Vafa, Witten 84')

And also *explicitly broken* after $U(1)_A$ breaking in the SM.
Chiral transformation shifts $\theta$ as $e^{i\alpha Q_5}|\theta> = |\theta + \alpha>$
With complex quark masses, a chiral transformation on quarks add $Arg\ det(M_q)$

$$\bar{\theta} = \theta_{QCD} + Arg\ Det\ M_q$$

Is the total angle, which breaks *P* and *T* (thus *CP* breaking), and naturally $\bar{\theta} \sim O(1)$.

$\bar{\theta}$ is an independent parameter of the theory (SM).
It is invariant under the anomalous symmetry:

$$U \to e^{i\alpha} U, \qquad \theta \to \theta - 2\alpha, \qquad M \to e^{-i\alpha} M$$

$\bar{\theta}$ in-principle only determined via measurement.
`Naturally' the combined $\bar{\theta}$ should take O(1) values.

For a conceptual review, see "*Reflections on the Strong CP Problem*", R. Peccei, hep-ph/9807514

In the effective strong interaction potential

breaks $U(1)_A$

$$\mathcal{L} = f_\pi^2 \,\mathrm{Tr}\, \partial_\mu U \partial^\mu U^\dagger + a f_\pi^3 \,\mathrm{Tr}\, MU + b f_\pi^4 \det U + h.c.$$

Yields the minimum at

$$V = -m_\pi^2 f_\pi^2 \sqrt{1 - \frac{4 m_u m_d}{(m_u + m_d)^2} \sin^2 \frac{\overline{\theta}}{2}}$$

$$\overline{\theta} = \theta + \theta_u + \theta_d$$

$$b = |b| e^{i\theta}$$

$$U = e^{i \frac{\Pi^a}{\sqrt{2} f_\pi} \sigma^a}$$

$$M = \begin{pmatrix} m_u e^{i\theta_u} & 0 \\ 0 & m_d e^{i\theta_d} \end{pmatrix}$$

# The strong CP problem

$\bar{\theta}$ causes CP-violation and appears in baryon EDM:

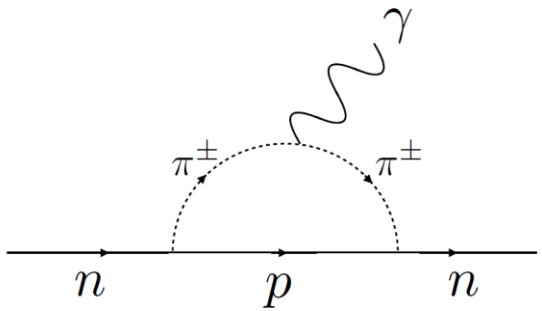


Feynman diagram for neutron EDM

$$\mathcal{L} = -\bar{\theta}\frac{c_+\mu}{f_\pi}\pi^a N\tau^a N^c - i\frac{g_A m_N}{f_\pi}\pi^a N\tau^a N^c, \qquad \mu = \frac{m_u m_d}{m_u + m_d}$$

$$d_n = \frac{e\bar{\theta} g_A c_+ \mu}{8\pi^2 f_\pi^2}\log\frac{\Lambda^2}{m_\pi^2} \sim 3\times 10^{16}\,\bar{\theta}\,\mathrm{e\ cm}$$

$g_A \approx 1.27$

$c_+ \approx 1.7$

1509.04411

Experimental value: $\bar{\theta} \lesssim 10^{-10}$

10 orders of fine-tuning.

Some easy ways out:

- massless *u*-quark (G 't Hooft, 76'): $m_u < 10^{-10} m_d$
- P-parity models (Babu, Mahapatra, 90')
- Spontaneous CPV models (Nelson,84' & Barr, 84')

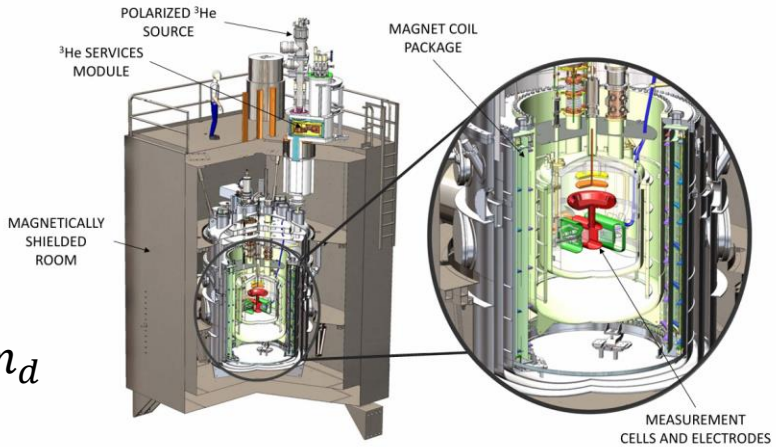


nEDM @ Oak Ridge
see recent worldwide updates: 1810.03718
& Snowmass 2203.08103

# Peccei & Quinn's global U(1) symmetry

- After spontaneous breaking, leaves a goldstone
- Anomalous, contributes to a $U(1)_A$ rotation
- Acquires a mass (pseudo-goldstone) at low energy.


Peccei, Quinn, 77'

Assume a global $U(1)_{PQ}$ as good UV symmetry

$$Q_i/U_i^c/D_i^c/L_i/E_i^c \longrightarrow e^{i\alpha} Q_i/U_i^c/D_i^c/L_i/E_i^c \ ,$$
$$H_d/H_u \longrightarrow e^{-i2\alpha} H_d/H_u \ .$$

(as in original PQWW)

$U(1)_{PQ}$ breaks after `some' scalar (has PQ charge) gets a vev ~ $O(f_a)$, leaving out a goldstone field $a$. The goldstone can acquire an (ABJ) anomalous coupling term :

$\frac{a}{f_a} G\tilde{G}$ that effective `extends' $\bar{\theta}$ into a dynamic field $\mathcal{L} \supset \left(\frac{a}{f_a} + \theta\right) \frac{1}{32\pi^2} G\tilde{G}.$

$$\bar{\theta} \ \rightarrow \ \overline{\theta} = \theta + \theta_u + \theta_d + \frac{a}{f_a}$$

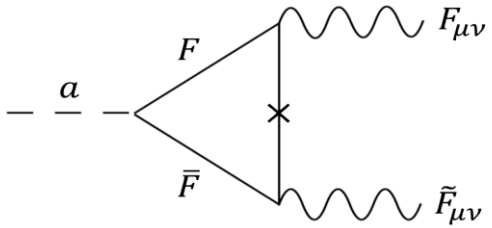


**KSVZ model** (Kim-Shifman -Vainstein-Zakharov):
heavy vector-like quarks, with coupling $\lambda_Q Q^c Q S$
Axion as the Im part of an extra scalar.
The PQ U(1): $Q^c/Q \to e^{i\alpha} Q^c/Q$, $S \to e^{-i2\alpha} S$

See Kim's review: *Rev.Mod.Phys.* 91 (2019) 4, 049902 (erratum)

**DSFZ model** (Dine-Fischler-Srednicki-Zhitnitskii):

$$\Delta L \supset \lambda H_u H_d S^2$$

$$a = \frac{1}{\sqrt{v_u^2 + v_d^2 + v_S^2}} (v_u \mathrm{Im} H_d + v_u \mathrm{Im} H_d + v_s \, \mathrm{Im} S)$$

$\{H_u, H_d, S\}$ charged as
{-1, -1, +1} under $U(1)_{PQ}$

$$f_a = \sqrt{v_u^2 + v_d^2 + v_S^2}$$

raised by large $S$ vev.

+ **Many other variants**, with a central goal to increase $f_a$ to avoid astro/flavor limits.
See review: The landscape of QCD axion models, *Phys.Rept.* 870 (2020) 1-117

Example: an effective UV construction into a Fraggett-Nielson $\left(\frac{S}{\Lambda}\right)^{n\geq 1} \bar{f}_i H f_j$ like :

A DSFZ type in case of $f$->SM fermions, e.g. can derive from GUT/higher scale physics, & realize some flavor features.

$$\Delta L \supset -y^u_{ij} Q_i U^c_j H_u - y^d_{ij} \frac{S}{M_*} Q_i D^c_j \tilde{H}_u - y^e_{ij} \frac{S}{M_*} L_i E^c_j \tilde{H}_u$$

$$Q_i, L_i, U^c_i, D^c_i, E^c_i : 1$$
$$H_u : -2$$
$$S : -4$$

*Mod.Phys.Lett.A* 37 (2022) 09, 2250055 + other PQ assignments

# Axion as cold dark matter

A fast oscillating field at the bottom of a $V(\phi)\sim(\phi-\phi_0)^2$ potential behaves as matter-like: $\rho(z) \sim (1+z)^3$

M. Turner, 83'

See axion cosmology review 1510.07633 & the more recent 2403.17697

axion starts to oscillate by $V_{inst}$.
after strong QCD phase transition

$$a(t) = a_0 \left(\frac{R_{m\sim H}}{R(t)}\right)^{2/3} \cos(m_a t)$$

**Misalignment Mechanism:**
axion potential overcomes Hubble friction and start oscillation from a homogeneous initial value $a_0$ (via inflation). Initial value gives the DM abundance:

$$\Omega_a h^2 \sim 2\times 10^4 \left(\frac{f_a}{10^{16}\ \mathrm{GeV}}\right)^{7/6} \langle\theta_{a,i}^2\rangle$$

( topological defects contribute if $f_a$ is lower than inflation scale)

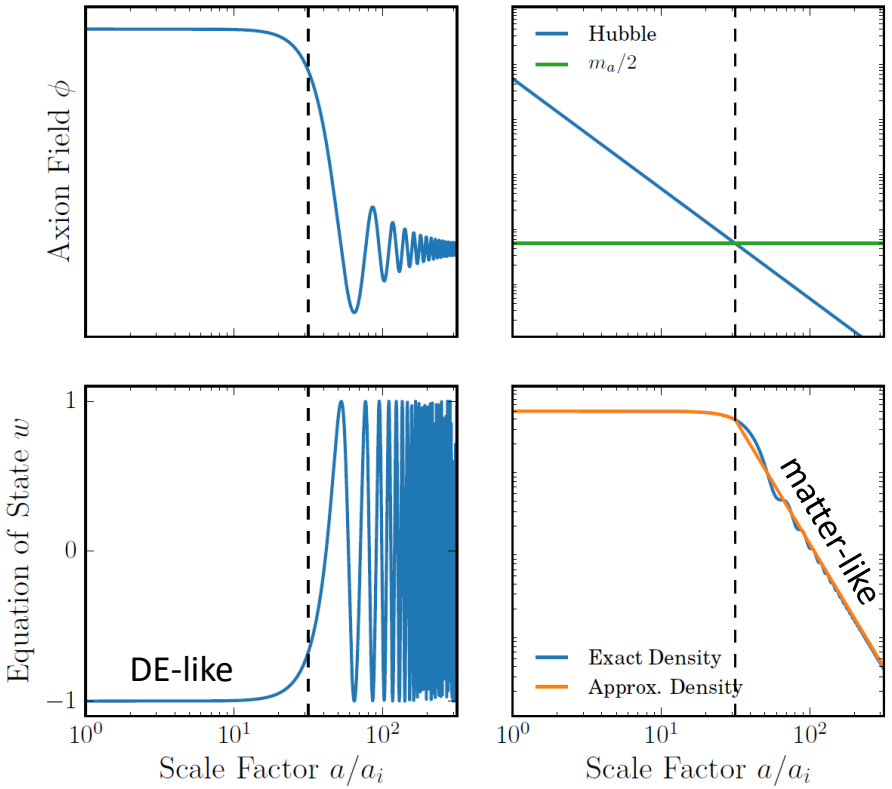

# Defects in post-inflation scenario

Cosmic strings form when U(1) breaks after end of inflation.

$$\phi(x) = (f_a + r(x))\, e^{i\theta(x)}$$

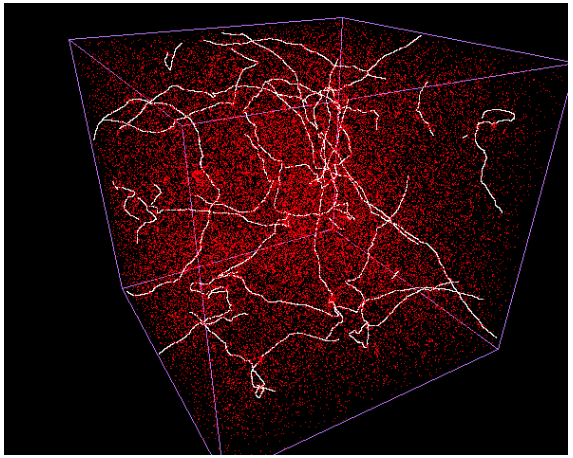

Domain walls form when $V_{QCD}$ develops a `true' vacuum (vacua)

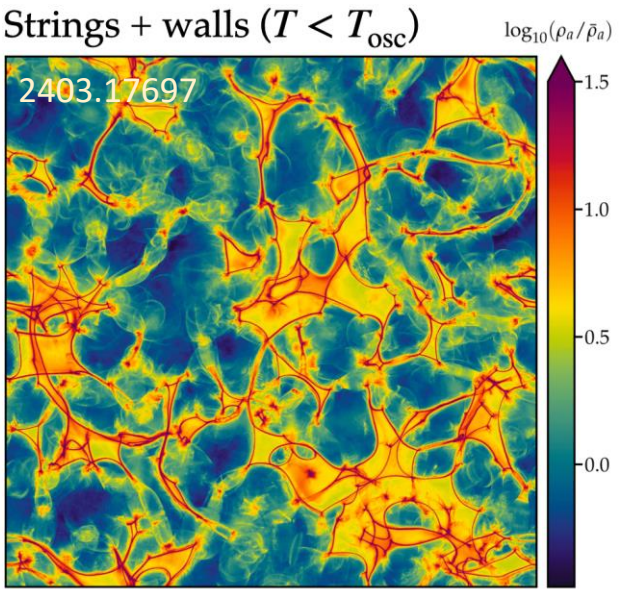


Contribute to the axion energy density:

$$\rho_a = \frac{1}{2} f_a^2 \dot{\theta}^2 + \frac{f_a^2}{2a(t)^2} (\nabla\theta)^2 + \chi(T)\,(1 - \cos\theta)$$

(DWs can unwind if $N_{DW}$=1)

Huge amount of numerical simulation devoted to study string networks, yet large uncertainties remain, see recent review by Saikawa, Redondo, et.al. 2401.17253

2403.17697

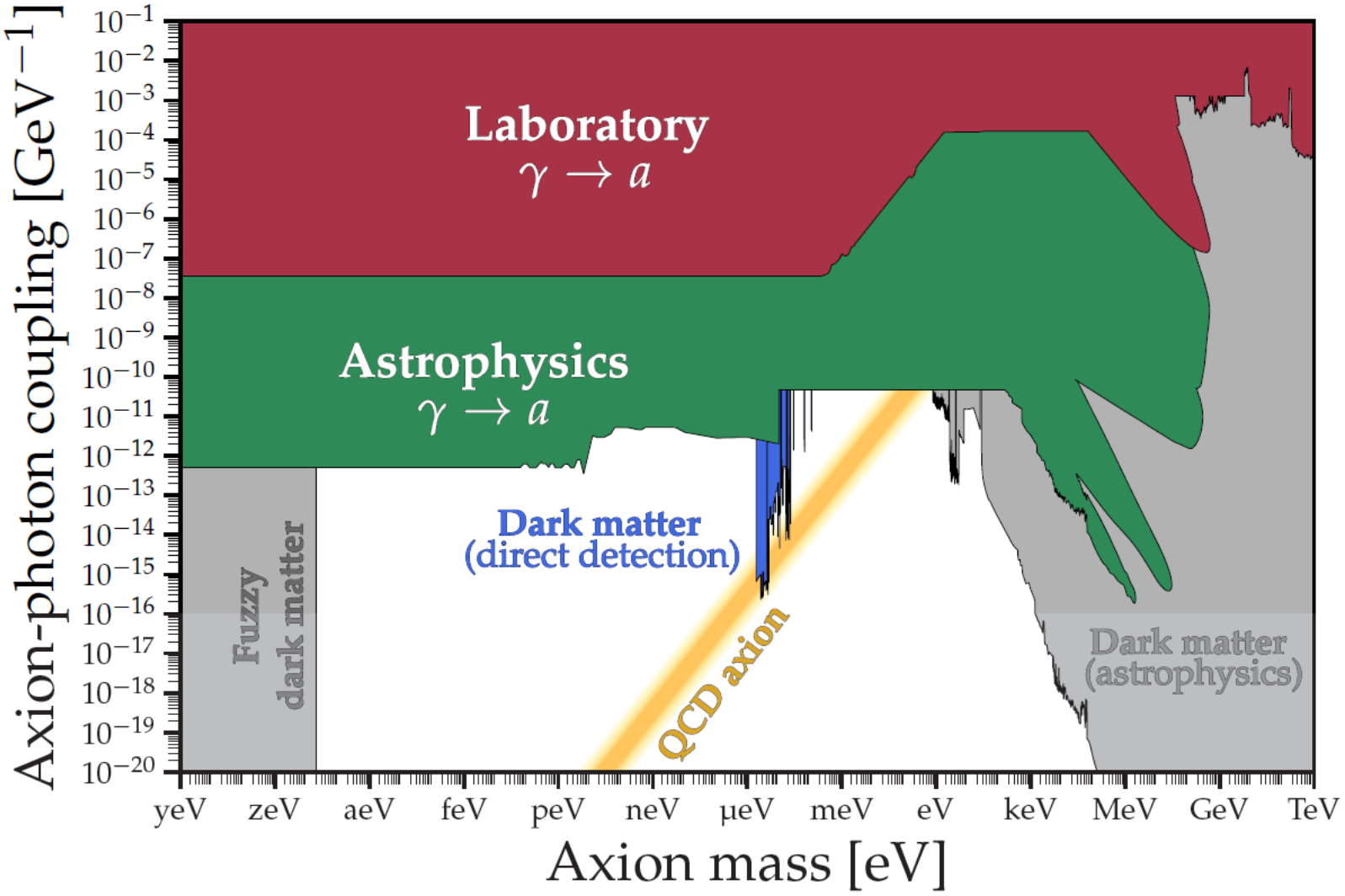
Laboratory
$\gamma \to a$
Astrophysics
$\gamma \to a$
Dark matter
(direct detection)
QCD axion
Fuzzy
dark matter
Dark matter
(astrophysics)
Axion-photon coupling [GeV$^{-1}$]
$10^{-1}$
$10^{-2}$
$10^{-3}$
$10^{-4}$
$10^{-5}$
$10^{-6}$
$10^{-7}$
$10^{-8}$
$10^{-9}$
$10^{-10}$
$10^{-11}$
$10^{-12}$
$10^{-13}$
$10^{-14}$
$10^{-15}$
$10^{-16}$
$10^{-17}$
$10^{-18}$
$10^{-19}$
$10^{-20}$
yeV
zeV
aeV
feV
peV
neV
μeV
meV
eV
keV
MeV
GeV
TeV
Axion mass [eV]

# Wavy Dark Matter form Objects

Pic. from 2203.10100

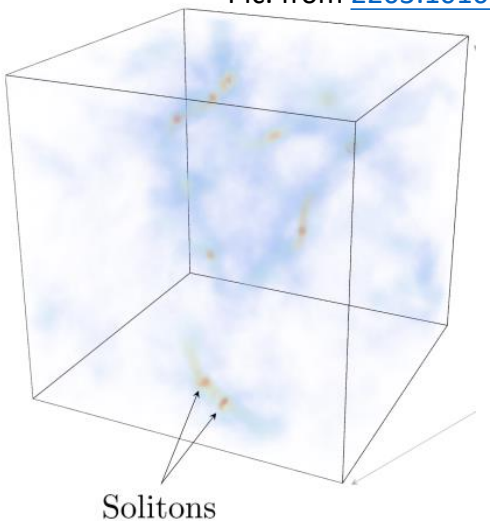


Ultra-light dark matter bosons form localized structures under gravity or self-interaction

(boson stars, etc.).

The Schrodinger-Poisson (SP) equation

$$i\,\dot{\psi} = -\frac{\nabla^2\psi}{2m} - Gm^2\,\psi\int d^3x'\frac{\psi^*(\mathbf{x}')\psi(\mathbf{x}')}{|\mathbf{x}-\mathbf{x}'|} + \frac{\partial}{\partial\psi^*}V_{nr}(\psi,\psi^*)$$

See Braaten & Zhang, 19' for a nice review

`Fuzzy DM', Lam Hui, 1610.08297

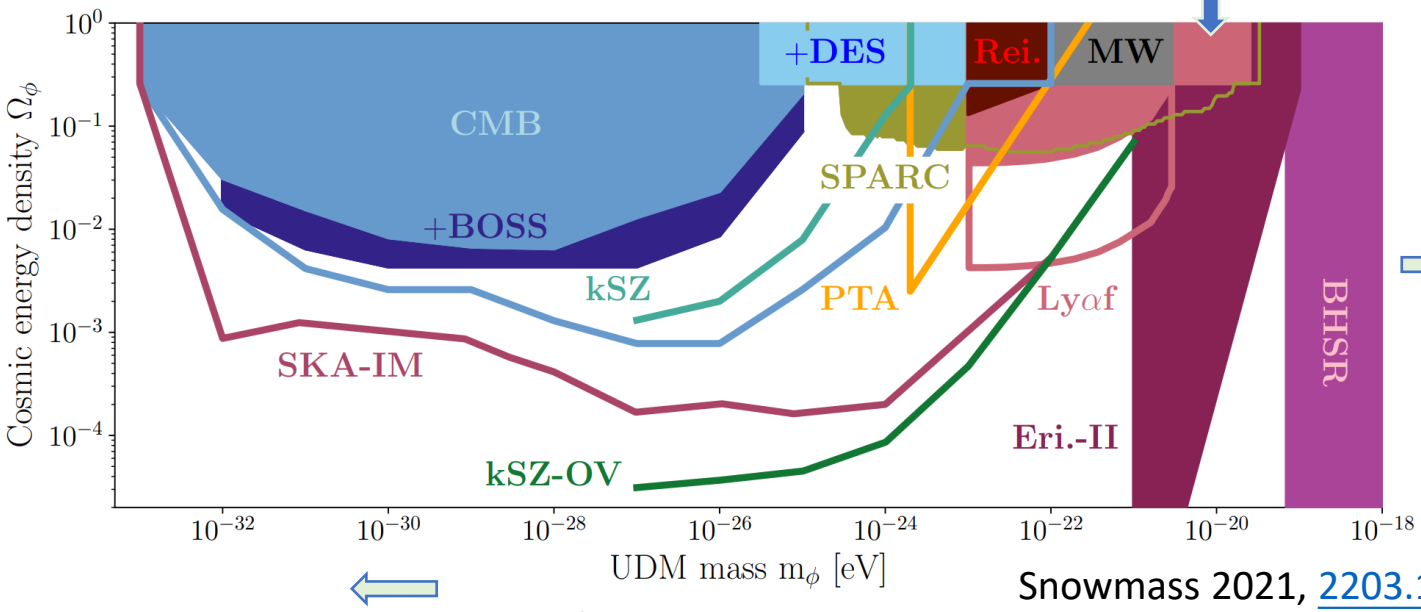


Sub-halo sizes

Lab exp. colliders

Cosmic scale

Snowmass 2021, 2203.14915

For binary evaporation, we repeat for the relative velocity $\Delta\vec{v}_r = \Delta\vec{v}_1 - \Delta\vec{v}_2$

**1st term** in energy increment:

$$\frac{\vec{v_r}\cdot\langle\Delta\vec{v_r}\rangle}{T} = -\frac{1}{2}\int\frac{(\vec{k}\cdot\vec{v_r})\vec{k}^2 d^3k d\omega}{(2\pi)^3}C_\Phi(\vec{k},\omega)\left(K_T'(\omega-\vec{k}\cdot\vec{v}_1)-K_T'(\omega-\vec{k}\cdot\vec{v}_2)\right)$$

$$= -\frac{1}{2}\int\frac{(\vec{k}\cdot\vec{v_r})\vec{k}^2 d^3k d\omega}{(2\pi)^3}C_\Phi(\vec{k},\omega)\left(\delta'(\omega-\vec{k}\cdot\vec{v}_1)-\delta'(\omega-\vec{k}\cdot\vec{v}_2)\right)$$

For $v_1 \approx v_2 \approx v_{CM}$ and $|v_1 - v_2| \ll v_{CM}$, this contribution is suppressed by $v_r / v_{CM}$

The evaporation will be dominated by the 2nd order $(\Delta v)^2$ term.

# Construction of the potential

An randomly distributed ensemble of solitons:

$$\rho(\vec{x},t) = \sum_i |\varphi(\vec{x}-\vec{x}_i-\vec{v}_i t)|^2 - \langle\rho\rangle$$

Soliton profiles are typically solved from S-P equation. Sample ansatzes:

$$\varphi(r) = \begin{cases} \frac{m_s^{\frac{1}{2}}}{(2\pi R^2)^{\frac{3}{4}}} e^{-\frac{r^2}{4R^2}}, & \text{Gaussian [27];} \\ \left(\frac{3m_s}{\pi^3 R^3}\right)^{\frac{1}{2}} \operatorname{sech}\left(\frac{r}{R}\right), & \text{Sech [16];} \\ \left(\frac{m_s}{7\pi R^3}\right)^{\frac{1}{2}} \left(1+\frac{r}{R}\right) e^{-\frac{r}{R}}, & \text{Exponential linear (EL) [16].} \end{cases}$$

normalized so that the density of the scalar field satisfies $\rho(r) \propto \varphi(r)^2$

# The Hamiltonian

Kinetic energy $$H_{\rm kin} = \frac{1}{2m_a}\int d^3x\, \nabla\psi^* \cdot \nabla\psi$$

(Self) Gravitational energy $$H_g = -\frac{Gm_a^2}{2}\int d^3x \int d^3x' \, \frac{|\psi(\vec{x},t)|^2 |\psi(\vec{x'},t)|^2}{|\vec{x}-\vec{x'}|}$$

Self-interaction energy $$H_i = \frac{\lambda}{16m_a^2}\int d^3x\, |\psi|^4$$

Static solution: $\psi(\vec{x},t) = \Psi(r)e^{-i\epsilon t}$ Ansatz: $\Psi(r) = \sqrt{\frac{3N}{\pi^3 R^3}}\,\mathrm{sech}\left(\frac{r}{R}\right)$

[From Zihang Wang's slides]
formulae adapted from Schiappacasse & Hertzberg, 18'

# Mass-radius relation of dilute axion stars